2021

Study of High-Performance Engineering Polymers Applied In Reciprocating Hermetic Refrigeration Compressors

Roger Nelson
Solvay Specialty Polymers, Roger.Nelson@Solvay.com

Patrick Kunc
Solvay Specialty Polymers

Laurent Hazard
Solvay Specialty Polymers

Celso Kenzo Takemori
Vibroacustica Development and Research, Brazil

Diego Willian da Silva
Vibroacustica Development and Research, Brazil

See next page for additional authors

Study of High-Performance Engineering Polymers Applied in Reciprocating Hermetic Refrigeration Compressors

Roger Nelson[1]*, Patrick Kunc[1], Laurent Hazard[1], Celso Kenzo Takemori[2], Diego Willian da Silva[2], Edmar Baars[2], Gustavo Rafael Bernardes [2], Luis Miguel Valdes Lopez[2]

[1]Solvay Specialty Polymers
Alpharetta, GA, United States of America
roger.nelson@solvay.com

[2]Vibroacustica Research and Development,
Joinville, SC, Brazil
celso@vibroacustica.com.br

*Corresponding Author

ABSTRACT

Manufacturers of hermetic refrigeration compressors for domestic and commercial applications have been increasing the energy efficiency of their products systematically over the last decades through the continuous efforts of in-house research groups, universities and suppliers. This joint effort encompasses the technical fields of design, materials, processes, manufacturing, and simulation techniques, to achieve a multidisciplinary approach to compressor optimization as applied to refrigeration systems. Gains such as increased efficiency of the electric motor, reduction of bearing friction power loss, minimizing back flow on valves have already been addressed and the continuous search for new approaches have been proposed. This work presents a study of energy efficiency gain by comparing low conduction heat transfer plastic materials to metallic materials used in current compressor designs. The components compared include the cylinder head, discharge muffler, shock loop, valve plate and crankcase. The energy efficiency gain was evaluated using the Coefficient of Performance (COP) through the use of the Conjugate Heat Transfer (CHT) model using superheating temperature. The CHT model temperature results were compared with the values measured by an instrumented compressor. To complement the study, the parts and assemblies were structurally evaluated using the finite element method under performance and durability test operating conditions. The feasibility of the mold filling process was verified, because the final design of the components must be a compromise between functional requirements and process solution. In conclusion, the results show that significant efficiency gains can be achieved through the use of engineering thermoplastic. This is achieved through careful material selection and proper design that considers not only material properties, but material and process costs using the flexibility of injection molding to group parts and subsystems.

1. INTRODUCTION

After several years of progress of increasing electric motor efficiency and reducing valve losses, the superheating inside the compressor remains an area where energy efficiency improvement can be made. Refrigerant superheating from the suction tube to the cylinder decreases the cooling capacity and the efficiency of a compressor. An excessive temperature can also degrade oil lubrication properties and may result in catastrophic failure of the compressor. There are three main heat sources inside the compressor: 1). The conversion of the electric energy into mechanical energy is not 100% efficient, so a portion is converted into heat inside the compressor, mainly in the stator and the coils. 2) The friction between moving/rotating parts and stationary parts, for example the crankshaft and crankcase and the piston and cylinder walls. 3) The compression process itself. It is not exactly a heat source, but the compression process heats up the refrigerant that enters inside the cylinder, and after being discharged the hot gas flows inside the compressor exiting the compressor and releasing heat energy to the compressor internal parts, i.e., cylinder head, valve plate, discharge muffler, shock loop, and crankcase.

One method to improve the thermal performance of a compressor, or decrease the superheating, is increase the thermal insulation between the hot and cold parts. This can be achieved by decreasing the thermal conductivity of the solid parts like the cylinder head and the discharge tube. There are several methods to estimate the effect of the thermal conductivity on the temperature distribution on the compressor. Lacerda and Takemori (2016) summarized the main works about the heat transfer models applied to compressors in twelve methods, that are a combination of (i) steady state or transient, (ii) partial compressor or full compressor and (iii) lumped model (0D), full three-dimensional model (3D) and 0D & 3D model.

In this work a full three-dimensional heat transfer model is employed, where the fluid domain is modeled by the tridimensional transient Navier-Stokes equations, while the solid domain is governed by the Fourier's Law. Based on that mathematical model, this work studies the efficiency variation if the thermal conductivity is decreased by replacing the current metallic components with polymeric parts. As mentioned before, some data is needed to perform the heat transfer simulation including the mass flow rate, the friction losses and the electric motor losses. For the mass flow rate, the method described in Ussyk (1984) is implemented in the commercial code GT-SUITEmp (GT-SUITE 2018). The friction losses are calculated using the established model of Reynolds equation for journal bearings as described in Raimondi and Boyd (1958) and Hamrock (1994). The electric motor losses are based on values found on the specialized literature, Diniz (2018).

2. METHODOLOGY

2.1 Compressor Selection and Reverse Engineering

For this work an after-market compressor was purchased. The selection criterion was a high efficiency household freezer refrigerator system based on the Brazilian energy efficiency rating program Inmetro (2018). The selected model is a variable speed R600a compressor whose speed ranges from 1620 to 4800 RPM. To build the 3D geometries needed for the numerical simulations, the compressor was disassembled, and parts were 3D scanned using optical and tomography methods. The part dimensions were measured using calipers and micrometers. Part weights were measured using a precision scale. Figure 1 shows the 3-D scan for the crankcase. The measured and calculated weights for all parts are shown in Table 1.

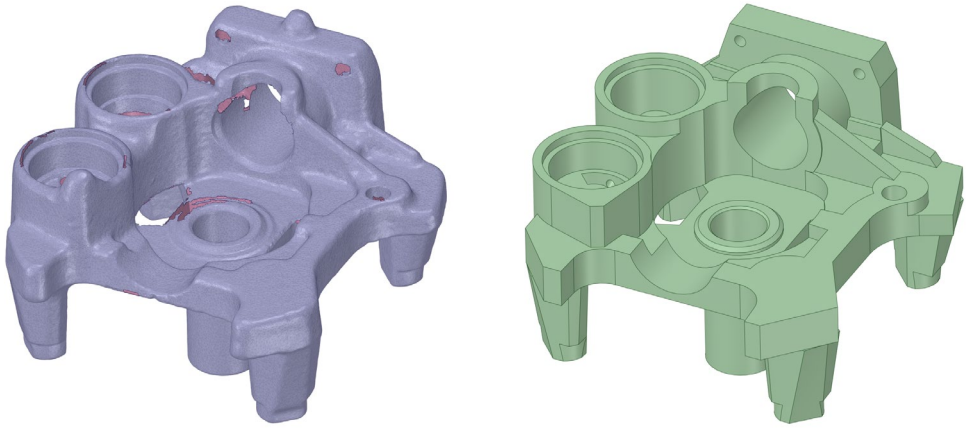

Figure 1: Crankcase. Left: 3D scan STL. Right: CAD geometry.

Table 1: Compressor Parts Mass

Part	Measured [g]	CAD [g]
Crankcase	1438	1421
Connecting Rod	17.5	20
Cylinder Head	45	46
Piston	44	45.6
Shell	2502	2536

2.2 Polymer Selection

The process of selecting suitable polymers for compressor components requires evaluating all the operating requirements, environmental conditions, ease of processing, and cost. As most polymers are thermal insulators, with thermal conductivities several orders of magnitude less than aluminum, the other factors become paramount. From a structural standpoint, the polymer must be able to withstand the high pressures and loads at elevated temperature over long lifetimes. This requires a polymer with good retention of mechanical properties at high temperature and good dimensional stability for creep and fatigue resistance. These requirements dictate that fillers be used. In addition, these properties must be maintained when exposed to the various refrigerants encountered in a compressor, so chemical resistance is required. Pai-Paranjape (2014) has demonstrated that certain filled engineering thermoplastics have good chemical compatibility with R-134A and R-410A compressor environments. Another material characteristic is the ability to be easily injection molded into complex components and maintain tight dimensional tolerances. The selected polymer must not be overpriced as to exclude its use.

When all the above are considered, the candidate materials are limited to a few engineering thermoplastics. Two semi-crystalline aromatic polymers which are excellent candidates are polyphenylene sulfide (PPS) and polyphthalamide (PPA). The selected compounds studied in detail are a 45% glass filled PPA and a 65% glass/mineral filled PPS. Not only do they meet the requirements needed for compressor components, but they are also cost competitive. Relevant mechanical and physical properties are listed in Table 2. [Solvay Specialty Polymers 2020]

Table 2: Properties Relevant to Compressor Components

Material	45% GF PPA	65% G/M PPS	Cast Aluminum
Thermal Conductivity (W/m.K)	0.328	0.49	160
Mold shrinkage (Flow / Cross flow) (%)	0.2 / 0.6	0.2 / 0.4	
Density (g/cc)	1.56	1.94	2.7
Tensile Modulus (GPa) @ 23°C	16	19	69
Tensile Modulus (GPa) @ 75°C	13	16.5	
Tensile Modulus (GPa) @ 120°C	10.5	10.3	
Tensile strength break (MPa) @ 23°C	263	165	317 ult, 160 yield
Tensile strength break (MPa) @ 75°C	185	141	
Tensile strength break (MPa) @ 120°C	125	100	
Poisson's ratio	0.4	0.34	0.33
Fatigue strength at 23°C 10E6 cycles (MPa)	82	83	105

2.3 Three-dimensional heat transfer model

As described in Lacerda and Takemori (2016), this model considers a full three-dimensional compressor geometry, Figure 7, with a steady state mass flow rate. This model also considers both fluid flow and solid parts. The solid parts are the suction tube, electric motor windings, connecting rod, counterweight, crankcase, crankshaft, cylinder gasket, cylinder head, cylinder head gasket, discharge covers, discharge valve stopper, discharge tube, piston, piston pin, rotor magnets, rotor, shell, shock loop, stator, suction muffler, valve plate, and oil (it is considered as a solid part, considering only the heat conduction). The suction fluid domain starts at the beginning of the suction tube and ends at the suction port through the suction muffler, Figure 2. The discharge fluid domain starts at the discharge port and ends at the end of the discharge tube, Figure 3. All interfaces are considered in such a way that the heat can flow between both fluid and solid domains. A total of 66 interfaces were considered.

A steady mass flow rate is applied to the suction port and to the beginning of the suction tube based on a pressure and temperature of 0.63 bar and 32 °C, respectively. The same mass flow rate is applied to the discharge port with a temperature T_D that follows Equation 1. The compression process is not solved but modeled evaluating the temperature increase from the beginning of the compression process when the refrigerant enters inside the cylinder until the time the gas is discharged out of the cylinder through the discharge port following an isentropic process. The temperature T_S is the mass flow averaged temperature on the suction port. The discharge pressure at the end of the discharge tube is 7.62 bar.

$$T_D = 0.98 \cdot T_S + 73.717 \tag{1}$$

To consider the induced flow by the rotating parts and the oil circulation inside the compressor, a momentum source term was used inside the compressor cavity, Figure 6. Using the momentum source term, it was possible to analyze the system without the need of solving a transient and multiphase model and increase the computational cost by orders of magnitude. An equivalent heat transfer coefficient, h_{eq}, is used on the shell external surface to consider both the convection and radiation effects, Equation 2. The value h_0 is calculated by setting the variable h_{eq} based on Dutra (2010).

Frictional losses are added to the pressure-volume power diagram to obtain the shaft power with the electric motor and inverter (controller) efficiency, making it possible to estimate the power consumption of the compressor. The values for the electric motor efficiency were extracted from Diniz (2018). The electric motor losses, Figure 4, are equally divided into the stator and windings losses. The friction losses, Figure 5, are applied on the following interfaces: crankshaft and crankcase, crankshaft and connecting rod, connecting rod and piston pin, piston pin and piston, and piston and cylinder, Lacerda and Takemori (2016). Figure 10 and 11 shows the results for the current research project.

$$h_{eq} = h_0 + \varepsilon\sigma\left({T_{shell}}^4 - {T_\infty}^4\right) \tag{2}$$

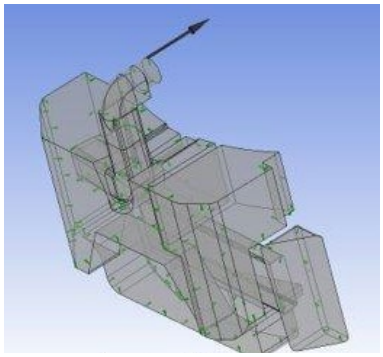

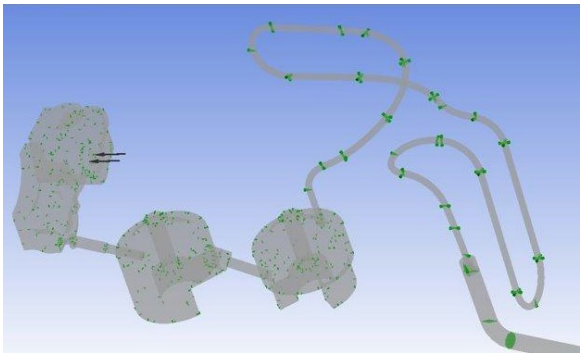

Figure 2 & 3: Suction fluid domain inside the suction muffler and discharge fluid Domain

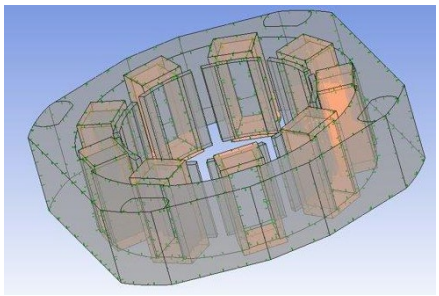

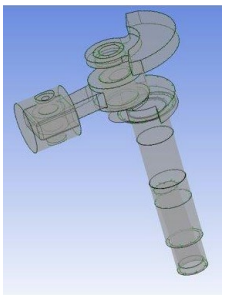

Figure 4 & 5: Electric motor solid domain, showing the windings and stator heat sources and the heat from friction losses are applied to the shaft, connecting rod and piston.

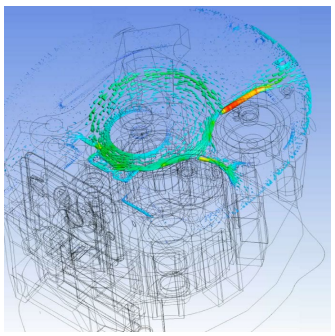

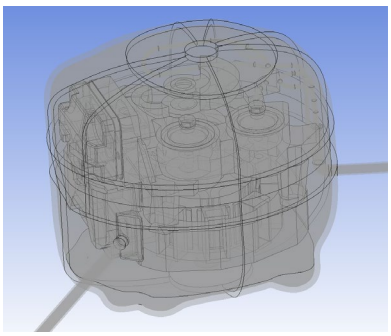

Figure 6 & 7: Momentum source term induces flow velocity inside the cavity showing velocity vectors on a horizontal plane. Full three-dimensional compressor geometry.

2.4 Experimental Setup for Temperature Measurement

Temperatures were measured at 14 locations on the compressor using K type thermocouples. Figure 8 shows an overview of the instrumented compressor. An accelerometer, the black wire connection in Figure 8, was attached to the shell to measure the rotational speed using the acceleration signal. Figure 9 shows how the thermocouples were attached to the compress.

Figure 8: Overview of the compressor with the thermocouple wires.

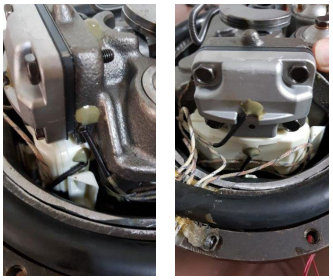

Figure 9: Thermocouples attached to the crankcase, suction muffler and cylinder head.

3. RESULTS AND DISCUSSION

Simulations showing the various effects of the momentum source term can be visualized in Figure 10 for a given rotational speed. In both charts the blue line are the measured values, and the orange ones are the simulation results. The chart on the left shows the simulation results without the momentum source term, while the chart on the right shows the results with it. Differences are expected as the experiment has uncertainties and a large metal flange that is absent from the simulation. The momentum source term improved the correlation between the simulation and the experiment. Figure 11 shows the comparison for three different rotational speeds with the momentum source term.

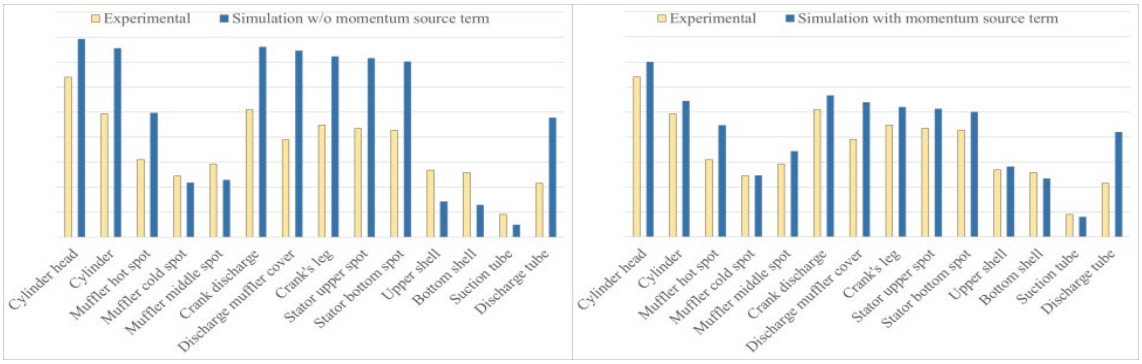

Figure 10: Temperature comparison between the measured and simulated values: Left chart is simulation **without** momentum source term. Right chart is simulation **with** momentum source term.

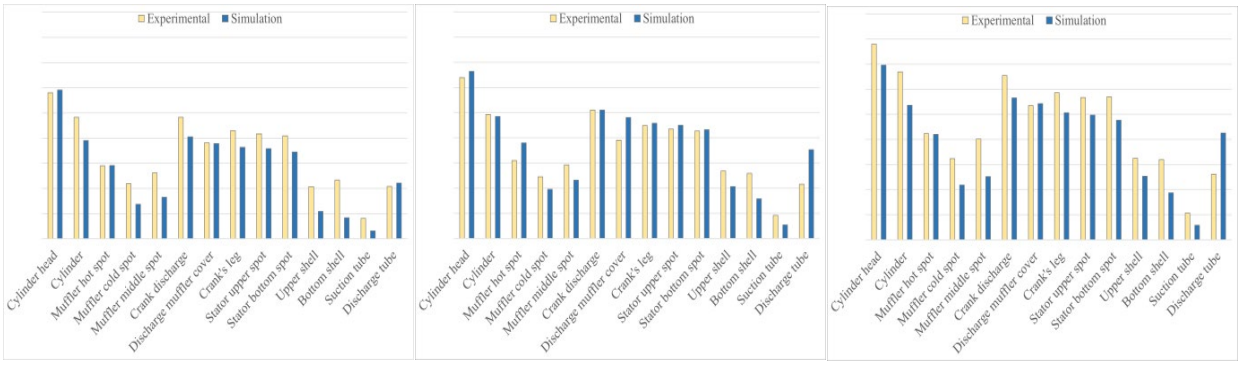

Figure 11: Temperature comparison between instrumented experimental compressor and simulation with momentum source term at three different rotational speeds: Low speed-left chart, Mid speed-middle chart, High speed-right chart

The 3D Heat Transfer Model temperature predictions closely mimic the temperatures measured in the instrumented compressor. This provides confidence, within limits, that this model's simulations can accurately predict temperatures that can be used to estimate the performance parameters in a compressor. Based on these thermal predictions, compressor efficiencies can be calculated and compared to estimate efficiency gains in a compressor by replacing metal components with polymeric materials, PPS and PPA, as suggested in the Polymer Selection section. Table 3 shows the efficiency gain when the thermal conductivity of metallic parts is replaced by the thermal conductivity of polymers. With polymers, the density of the fluid refrigerant that enters in the cylinder increases, resulting in an improvement of the cooling capacity and efficiency. The efficiency gain presented in the table below is estimated based upon the increase in the fluid refrigerant density.

Table 3: Polymer studies and results

Compressor part	Baseline	Case 01	Case 02	Case 03	Case 04	Case 05	Case 06
Cylinder Head	Metal	Polymer	Polymer	Polymer	Polymer	Polymer	Polymer
Shock loop	Metal	Metal	Polymer	Polymer	Polymer	Polymer	Polymer
Crankcase	Metal	Metal	Metal	Polymer	Metal	Polymer	Polymer
Valve Plate	Metal	Metal	Metal	Polymer	Polymer	Polymer	Polymer
Discharge Tube	Metal	Metal	Metal	Metal	Metal	Polymer	Polymer
Discharge Muffler Covers	Metal	Metal	Metal	Metal	Metal	Metal	Polymer
Efficiency Gain	0.00%	0.47%	0.64%	1.65%	0.83%	1.95%	2.10%

4. STRUCTURAL ANALYSIS

The cylinder manifold consists of the cylinder head, cylinder head gasket, valve plate, suction reed valve, valve plate gasket and crankcase. Those components are assembled to ensure tightness and define the cylinder's clearance volume, which is closely related to the efficiency of the compressor. The temperatures of the compressor components were determined by the CHT analysis for the baseline and were compared with experimental data. The plastic material properties were reduced to account for the elevated temperatures as shown in Table 2. The effect of temperature is shown for selected properties such as tensile modulus, strength, and the fatigue limit. The characterization of the NI-2085, an NBR binder gasket material, which is largely used by compressor manufacturers, is made by a special compression rig test where the deformation versus load is determined and used in finite element programs through the deformation versus pressure relationship.

In the analysis, three load steps were applied (see Figure 12):

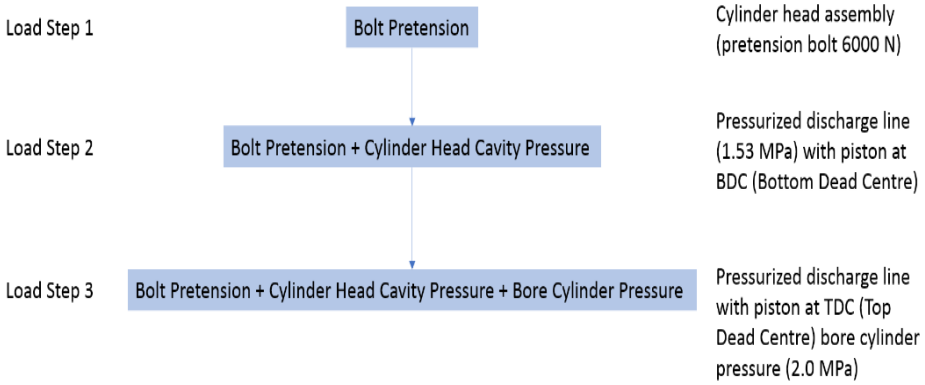

Figure 12: Load steps for structural analysis

The structural simulation of the baseline compressor, Figure 13, verified stress concentrations in the region of the fillet radius of the bolt head seat, Figure 14. A sensitivity analysis was performed and it was found that even by reducing this stress concentration by increasing the radius the resulting stresses were still too high for the plastic material. This indicated a geometrical change would be necessary.

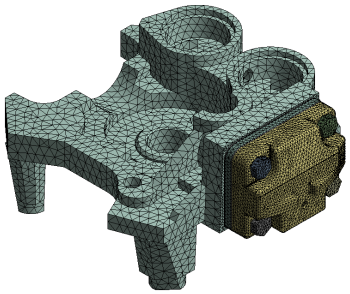

Figure 13: Baseline version - Mesh of cylinder manifold components.

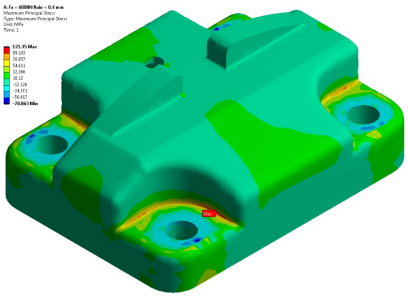

Figure 14: Stress concentration at fillet radius on recess of bolt head seat.

The strategy for obtaining a plastic cylinder head was to reduce the stress concentration in the filleted region since the stress values in the rest of the part were compatible with the plastic material properties considered for the application. In Figure 15 we show the evolution of the alternatives, starting with the simplest model (Version 1), in which the cylinder head was a rectangular solid object with a flat top surface where the stress concentrator is eliminated. The following designs were optimized for stiffness, improved processability, and weight reduction.

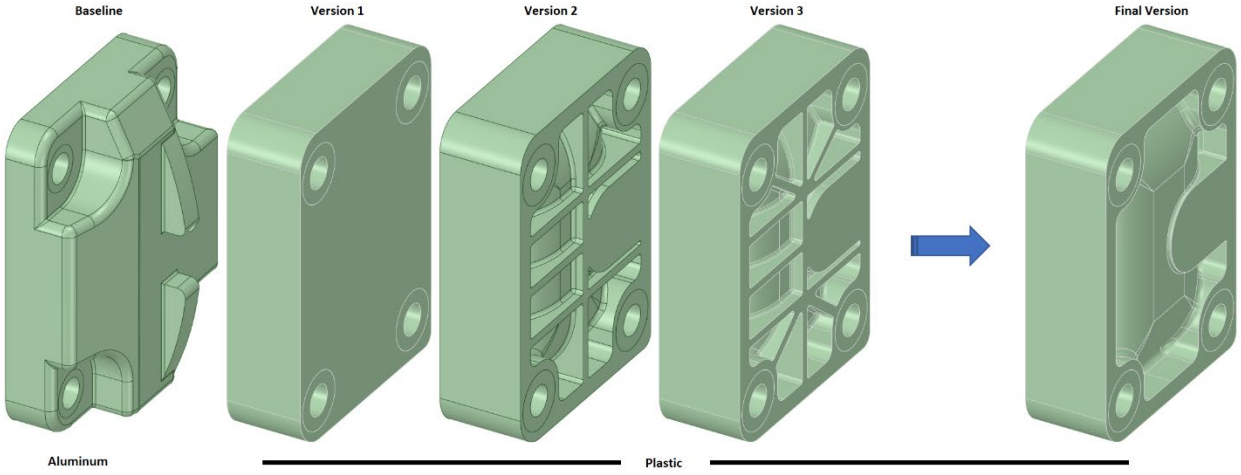

Figure 15: Geometry of cylinder head from baseline to plastic final version

The same loads were applied to the optimized model of the plastic cylinder head. The region of maximum tensile stress has changed, and the value is much lower than that found in the aluminum cylinder head, see Figure 16. The results in the Goodman-Haigh diagram, Figure 17, show that the cylinder head with the proposed geometry (Final Version) can be made of plastic and the stress level is compatible with the material. The average tension is high, but three times less than the aluminum cylinder head, and the alternating stress is still low. The adoption of a plastic cylinder head is a compromise between the geometry necessary to obtain the stiffness, contact pressure and the low mechanical stresses compatible with the material, and a robust process that can obtain parts without defects.

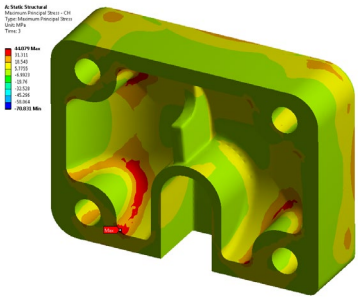

Figure 16: Stress results for load step 3 of plastic cylinder head

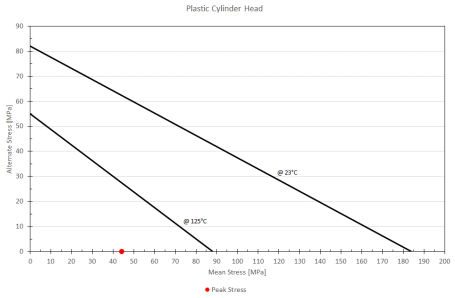

Figure 17: Goodman-Haigh diagram for cylinder head made of plastic

5. PROCESS MOLDING INJECTION SIMULATION

Since the most cost-efficient plastic production method for structural plastic parts is injection molding, this process was chosen for this study. Currently, cylinder heads are cast aluminum and in general the geometries used for casting are not suitable for a robust injection molded part. Injection molding simulations were performed on different geometries in order to find an optimized configuration that could both sustain the structural requirements and be easily injection molded. The original baseline geometry is shown in Figure 15. The wide variation in part thickness was not suitable for injection molding, so a cored-out version with ribs was initially analyzed, Figure 18. The injection point is shown. The partially filled cavity is shown in Figure 19. An uneven fill pattern is observed in Figure 19 caused by the thickness variation resulting in converging flow fronts at high stress areas. The converging flow fronts are called weld lines and the resulting strength in these locations are less than the nominal material. Several design iterations were made to reduce the severity of the weld lines and relocate them in lower stress areas, see Figure 15. The resulting flow pattern is shown in Figure 21.

The fiber orientation is shown in Figure 22. Areas of higher orientation are shown in red. Since the strength and stiffness of an injection molded part are influenced by the fiber orientation, it is important to know how the fibers are distributed throughout the part. This information can be readily transferred from the flow simulation to the structural analysis to fine tune the design. The predicted deformation or warpage of the part after molding is shown in Figure 23. Of special interest for the cylinder head is the flatness of the seal area. The variation should not be so great that it inhibits the gasket from sealing. As shown in this example, the overall variation in the out-of-plane displacement of the seal or flatness is .0025 mm. Note that this variation can be reduced by changing processing parameters, geometry, materials, and even accounted for with tooling modifications. The results show that it is possible to develop a geometry which can be readily injection molded and still withstand the service loads imposed upon it.

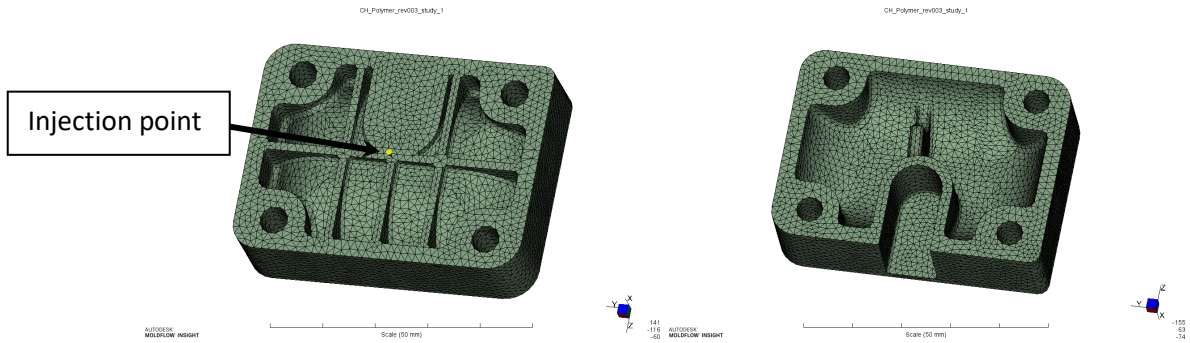

Figure 18: Finite element model

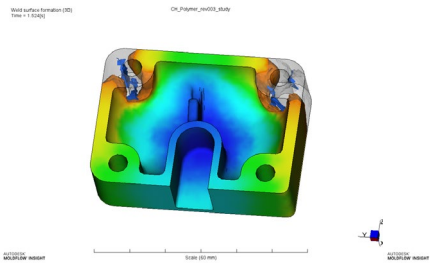

Figure 19: Fill pattern at 1.5 seconds with weld lines shown

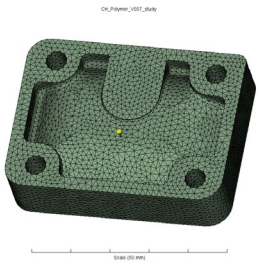

Figure 20: Optimized design eliminates critical weld line

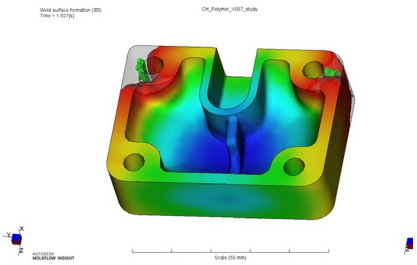

Figure 21: Fill pattern at 1.5 seconds with weld lines shown

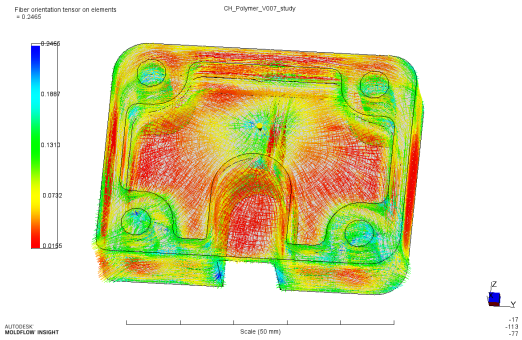

Figure 22: Fiber orientation

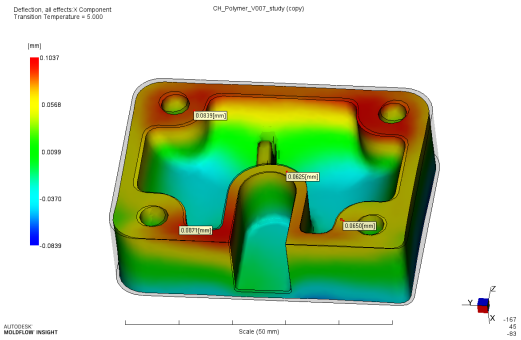

Figure 23: Deformation of seal surface (flatness)

4. CONCLUSIONS

Properly selected polymers, in particular those that maintain their high stiffness, strength and chemical resistance when exposed to compressor environments over long times, combined with the proper design to meet the physical properties requirements of the application, can replace metal components in reciprocating compressors, and increase a compressor efficiency. In this article, plastic alternatives for the cylinder head, valve plate, shock loop, crankcase, discharge tube, and discharge muffler cover were all evaluated for efficiency improvement. The use of structural analysis and mold flow simulation software can substantiate design modifications and increase the success of metal to plastic replacement. This was demonstrated by applying those techniques to a cylinder head made of die cast aluminum and replacing it with a 45% glass reinforced polyphthalamide PPA polymer.

The 3D Heat Transfer model accurately predicted the temperature profile of our instrumented reciprocating compressor and the addition of the momentum source term improved the temperature correlation between the instrumented compressor and the 3D Heat Transfer Model, thus providing a method to study the effects of semi-crystalline aromatic polymer replacement of metal components in reciprocating compressors and estimating the associated efficiency gains. This heat transfer model predicted compressor efficiency gains when the metal components were replaced with PPS and PPA materials. These polymers, primarily due to their lower thermal conductivity, increased the density of the refrigerant entering the cylinder resulting in an improvement of the cooling capacity and efficiency.

NOMENCLATURE

STL	Stereolithography file format
A_p	Pressure area
A_{eff}	Flow area
$\dot{m}$	Mass flow rate

ρ_{is}	Density at the throat
ρ_0	Upstream stagnation density
U_{is}	Isentropic velocity at the throat
C_D	Discharge coefficient
A_R	Reference flow area
P_R	Absolute pressure ratio (static outlet pressure/total inlet pressure)
R	Gas constant
T_0	Upstream stagnation temperature
γ	Specific heat ratio
h_{eq}	Equivalent heat transfer coefficient
h_0	Heat transfer coefficient
T_{shell}	Local shell external surface temperature
T_∞	External ambient temperature

REFERENCES

Raimondi, A. A., Boyd, J. (1958). A solution for the finite journal bearing and its application to analysis and design. ASLE Transactions.

Hamrock, B. J. (1994). Fundamentals of fluid film lubrication.

Ussyk, M. S. (1984). Simulação numérica do desempenho de compressores herméticos alternativos (in portuguese). Federal University of Santa Catarina, Department of Mechanical Engineering.

Lacerda, J. F., Takemori, C. K. (2016). CFD Approach to Evaluate Heat Transfer in Reciprocating Compressors. Proceedings of the International Compressor Engineering Conference.

INMETRO (2018), http://www.inmetro.gov.br/consumidor/pbe/refrigeradores.pdf, visited in March 2020.

Pai-Paranjape, V. (2014). Chemical Compatibility of High-Performance Engineering Thermoplastics in Compressor Environments. Proceedings of the International Refrigeration and Air Conditioning Conference

Solvay Specialty Polymers (2020)-Amodel® Design Guide https://content.solvay.com/amodel-ppa-design-guide

GT-SUITE Flow Theory Manual Version 2018 (2018), Gamma Technologies.

Diniz, M. C. (2018). Análise numeric-experimental de compressores alternativos em transientes periódicos típicos de refrigeradores domésticos (in portuguese), Federal University of Santa Catarina, Department of Mechanical Engineering.

ACKNOWLEDGEMENT